



This is a repository copy of *An experimental investigation of MOSFET intrinsic body diode performance*.

White Rose Research Online URL for this paper:  
<http://eprints.whiterose.ac.uk/144231/>

Version: Accepted Version

---

**Proceedings Paper:**

Petersen, A., Stone, D.A. [orcid.org/0000-0002-5770-3917](https://orcid.org/0000-0002-5770-3917) and Foster, M.P. [orcid.org/0000-0002-8565-0541](https://orcid.org/0000-0002-8565-0541) (2018) An experimental investigation of MOSFET intrinsic body diode performance. In: 2018 IEEE 27th International Symposium on Industrial Electronics (ISIE). 2018 IEEE 27th International Symposium on Industrial Electronics (ISIE), 13-15 Jun 2018, Cairns, QLD, Australia. IEEE , pp. 341-345. ISBN 9781538637050

<https://doi.org/10.1109/ISIE.2018.8433636>

---

© 2018 IEEE. Personal use of this material is permitted. Permission from IEEE must be obtained for all other users, including reprinting/ republishing this material for advertising or promotional purposes, creating new collective works for resale or redistribution to servers or lists, or reuse of any copyrighted components of this work in other works. Reproduced in accordance with the publisher's self-archiving policy.

**Reuse**

Items deposited in White Rose Research Online are protected by copyright, with all rights reserved unless indicated otherwise. They may be downloaded and/or printed for private study, or other acts as permitted by national copyright laws. The publisher or other rights holders may allow further reproduction and re-use of the full text version. This is indicated by the licence information on the White Rose Research Online record for the item.

**Takedown**

If you consider content in White Rose Research Online to be in breach of UK law, please notify us by emailing [eprints@whiterose.ac.uk](mailto:eprints@whiterose.ac.uk) including the URL of the record and the reason for the withdrawal request.



[eprints@whiterose.ac.uk](mailto:eprints@whiterose.ac.uk)  
<https://eprints.whiterose.ac.uk/>

# An Experimental Investigation of MOSFET Intrinsic Body Diode Performance

A. Petersen, D. A. Stone & M. P. Foster  
Centre for Research in to Electrical Energy Storage & Applications  
Electric Machines and Drives Research Group  
University of Sheffield, UK  
Email: apetersen1@sheffield.ac.uk

**Abstract**—In order to enable evaluation of power loss during both forward and reverse conduction of intrinsic body diodes in power MOSFETs, an experimental series is performed to derive a set of expressions to approximate performance. A set of relevant performance metrics are selected, and then tested over a range of devices. Any correlation between these metrics and properties of these devices commonly provided by device manufacturers are investigated and quantified. A set of empirical expressions are derived from the closest correlations found, that therefore enable an estimation of performance of the body diode without any prior testing, with a predicted margin of error.

## I. INTRODUCTION

As part of ongoing research, it became a point of interest to estimate performance of the body diode in power MOSFETs. This was in order to optimise converter design and device selection for minimum power loss, with a view to compare the performance of the body diode with use of external high performance switching diodes. It was quickly discovered that very few manufacturers provide information as to the performance of this part of this aspect of the device. The exceptions to this rule being the few devices designed with the body diode in mind, e.g. IXYS's HiPerFET series.

A review of the literature in this field yielded little of use. Existing discussion in literature focuses instead on the experimental exploration of a specific device (or very narrow range of devices) [1-4], or perhaps discussing a die-level model to predict some parameters [5, 6]. This is of little help in the derivation of a practical prediction from readily available information over a broad range of devices. Creation of such a prediction is therefore the goal of this paper.

Initially, the derivation of a model from die level and up may seem sensible, but this is impractical as manufacturers seldom provide even the most basic information about the device topology. The goal is, therefore, to explore the possibility of a correlation between relevant body diode performance metrics and readily available device parameters. The use of readily available parameters enables the comparison of many devices over a range of conditions at once without costly and time-consuming testing of large sets of devices.

An example of a situation in which this would be of great use is the optimisation of the design of  $N^{\text{th}}$  order multilevel

converters, as in [7], where one is less interested in what the performance of specific device is but instead what the performance of a device with given properties is likely to be.

## II. METHOD

### A. Device Selection and Testing Design

The first stage in development of the testing procedure is selection of devices to be tested. The key criterion in this process is to ensure confidence in there being a broad and even distribution of devices selected for testing. While the correlations with a number of parameters were considered, the two primary parameters are maximum drain-source voltage rating,  $V_{DS,MAX}$ , and maximum continuous drain current rating,  $I_{D,MAX}$ . Figure 1 shows the ratings of the devices selected for testing, showing a fairly even distribution over the majority of the range of ratings available in mainstream silicon power MOSFETs. A full list of devices selected for testing can be found in Appendix A.

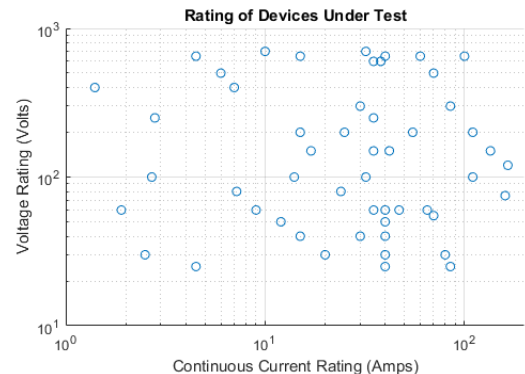


Fig. 1. Voltage and current rating of devices selected for testing series.

It was also necessary to consider what device parameters would be explored for their potential correlation with the relevant diode performance metrics. To do that the performance metrics must be selected, and to do that the sources of loss due to diode conduction in a power converter must be considered.

In an H-bridge converter the body diodes (assuming no external diodes are used) conduct forward as a flyback path during dead time, immediately followed by conduction in the opposite direction during reverse recovery. To estimate the

power loss depends on system parameters, of course, but a model of certain aspects of loss can be tied to specific performance metrics.

For a calculation of forward conduction power loss, the forward voltage of the diode for a given current must be known. This can be found from the body diode current-voltage curve (I-V curve). A diode I-V curve near its conduction threshold can be accurately modelled using the Shockley equation, but as performance near the conduction threshold of the body diode is irrelevant this is not an appropriate model. At higher current resistance dominates performance, and as such the body diode I-V curve is simplified to a linear model that is represented by an on-state resistance and a ‘simplified threshold voltage’. The comparison between actual test data and this approximation can be seen in figure 2.

Power loss during reverse conduction in, for example, an H-bridge converter, is due to the diode permitting conduction across the bridge as the opposite switching devices begin to conduct. This causes transient short-circuit current to flow across the bridge over a very short period – though dependant on system parameters this could be a significant issue. The device dependant performance metric is the amount of charge that must be removed from the saturated body diode before reverse conduction ceases. This is hereby referred to as the reverse recovery charge.

Therefore, the three body diode performance metrics to be experimentally explored are:

- body diode forward resistance,
- body diode simplified threshold voltage,
- and body diode reverse recovery charge.

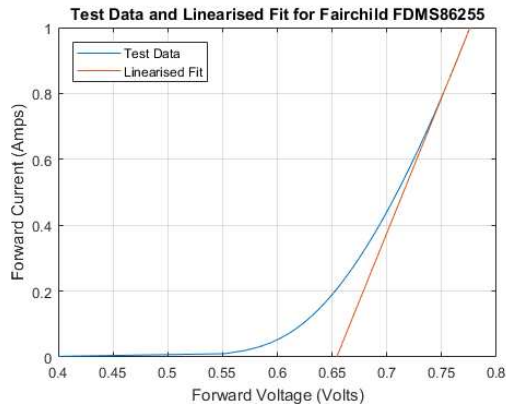


Fig. 2. Experimentally derived I-V curve of a MOSFET body diode plotted with its linearised approximation.

### B. Experimental Procedure

Over this set of devices (see Appendix A), the I-V curves were measured using a Keithley 2612A Sourcemeater. The curves were traced up to 1A, ensuring the linear region of the diode was reached. This permitted a linearised approximation to be used, that can be seen in figure 2. The instrument was configured to provide the desired current followed, after a short settling time (25ms), by a voltage

measurement and then an off period, for each of the samples taken. This was done with a low enough duty cycle (10%) to ensure negligible heating of the device. As such, any predictions made are of performance at room temperature.

Measurement of the reverse recovery current was performed with a custom testing platform which rapidly transitions a diode from conducting forward current to being reverse biased. A precise measurement of the current over time between reverse recovery starting and ending permits inference of the reverse recovery charge. In these tests the gate was tied to the drain to ensure the MOSFET remained completely off at all times.

To investigate how much noise is present on these measurements not only a single test on each device will be run but instead two units of each device will be tested three times each. This will permit independent investigation of the noise between multiple tests on the same unit and the noise between the performance of multiple supposedly identical units.

### C. Statistical Analyses

From this test series, the three key parameters describing body diode performance for each device are extracted: forward resistance, simplified threshold voltage, and reverse recovery charge.

These measured values are to be investigated for correlation with device parameters universally available through manufacturer datasheets. Voltage and current rating are two obvious parameters, but others were selected also. The datasheet parameters to be investigated for correlation with experimentally derived performance metrics are:

- maximum drain-source voltage rating,
- maximum continuous drain current rating,
- nominal threshold voltage,
- devices capacitances ( $C_{OSS}$ ,  $C_{ISS}$  and  $C_{RSS}$ ),
- and maximum package power dissipation.

The device capacitances and nominal threshold voltage are closely linked to die geometry, and therefore possibly correlated with the performance metrics of interest. The maximum power dissipation seemed worth investigating as this is representative of the ‘bulk’ of the device, though this is affected significantly by the package rather than just the properties of the die.

The capacitance values, which vary with respect to drain-source voltage, are all evaluated at 1V. The maximum power dissipation, which varies with temperature, is evaluated at the only temperature consistently available, 25°C.

The strength of correlation between the performance metrics and device parameters will be evaluated using the Pearson correlation coefficient. Upon inspection of test data, first order linear and logarithmic fits were explored. The noise of measurements, both between tests and between individual devices, will be expressed in terms of standard deviation from the mean.

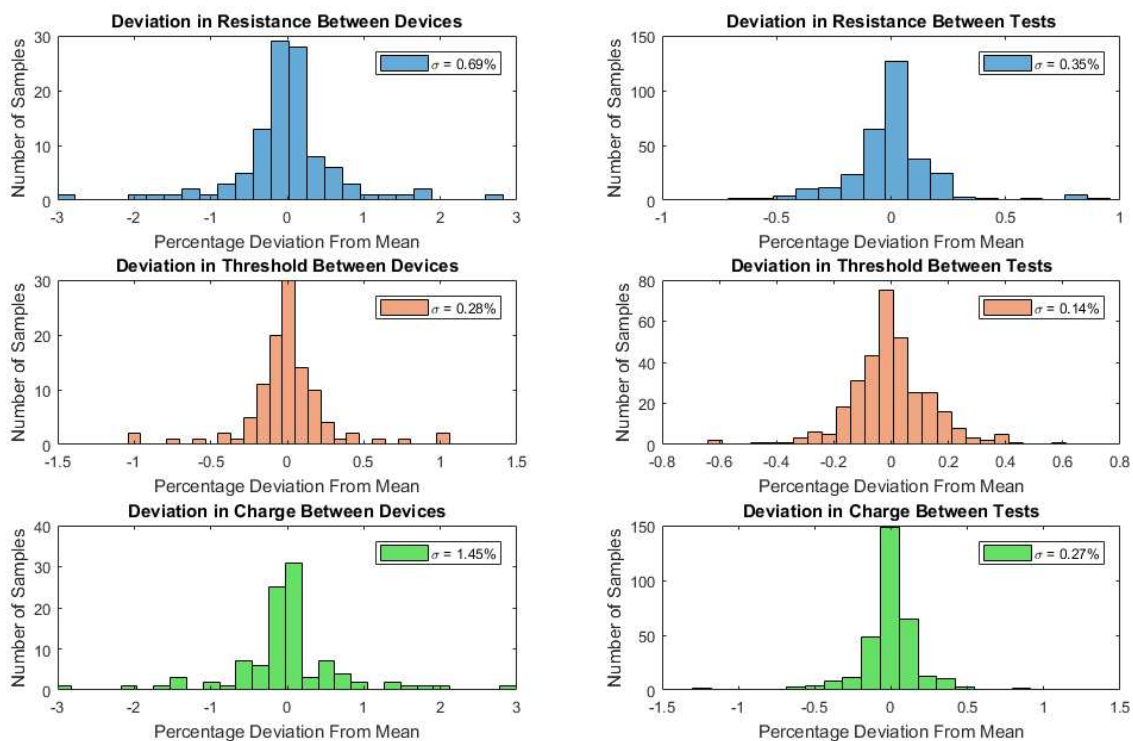


Fig. 3. Noise of experimental process: both between tests and between individual devices for three key body diode performance metrics. Both the distribution and the standard deviation ( $\sigma$ ) as a percentage of the mean are shown.

### III. RESULTS

When all experimental had been collected an analysis of the noise on these measurements was performed. The results of this are shown in figure 3. A key observation is that deviation between multiple tests on the same device is significantly lower than deviation between devices. This demonstrates that the testing methodology is sufficiently consistent as it does not increase uncertainty any more than the manufacturing tolerance of multiple supposedly identical devices. Furthermore, the distributions are approximately normal, as one might expect, further supporting the validity of testing as a skewed distribution might suggest a systematic source of error. Finally, the deviation is low overall, with even extreme outliers lying no more than 3% from the mean, thereby showing that the real performance of the devices is reasonably consistent.

Figures 4-6 show the modulus of the Pearson correlation coefficient between each of the selected device parameters for all four types of fit considered, for each body diode performance metric respectively. A 'log-x fit' (as seen in figures 4-6) describes a linear fit between the performance metric and the logarithm of device parameter. A 'log-y fit' is the opposite of this, and linear and log-log fits are self-explanatory.

While the Pearson correlation coefficient is normally expressed in the range -1 to 1, in this case only the strength of correlation is needed, so the modulus of this coefficient is used. Therefore, the coefficient that is normally in the range 1 to -1 is now in the range 0 to 1, with 1 representing perfect correlation and 0 representing no correlation.

Of the data shown in figures 4-6, the strongest correlations for each of body diode resistance, voltage and charge was chosen as the best fit. These fits are shown alongside the experimental results on suitable axes in figures 7-9.

Figure 7 shows the correlation between MOSFET drain-source voltage rating and body diode resistance, which has a correlation coefficient of 0.67. While this is the best correlation found for the diode resistance, it is notably weaker than the optimal for voltage drop and reverse recovery charge. This is still a very worthwhile estimation, and even with its shallow gradient it reduces the standard deviation of the error compared with taking a mean value from 21m $\Omega$  to 11m $\Omega$ .

Figure 8 shows the correlation between MOSFET input capacitance,  $C_{ISS}$ , and body diode simplified threshold voltage. This is the strongest correlation found for diode voltage with a correlation coefficient of 0.83, or more precisely -0.83 as it is a negative correlation. As with figure 7, note that the x-axis is labelled logarithmically to more appropriately display the type of fit.

Figure 9 shows the correlation between MOSFET output capacitance,  $C_{OSS}$ , and body diode reverse recovery charge. This is very good fit, with a correlation of 0.92 and few outliers. The fit in this case is not a log-x fit but rather a log-log fit, and as such the figure is plotted with both axes numbered logarithmically.

MOSFET device parameter	linear fit	log-x fit	log-y fit	log-log fit
Drain-Source Voltage Rating	0.61	0.67	0.59	0.67
Drain Current Rating	0.08	0.08	0.12	0.14
Nominal Threshold Voltage	0.55	0.51	0.55	0.51
$C_{OSS}$ (@1V)	0.16	0.41	0.17	0.45
$C_{ISS}$ (@1V)	0.27	0.29	0.30	0.34
$C_{RSS}$ (@1V)	0.28	0.43	0.29	0.47
Max Power (@25°C)	0.24	0.60	0.25	0.65

Fig. 4. Modulus of Pearson's coefficient of correlation between body diode forward resistance and MOSFET device parameters.

MOSFET device parameter	linear fit	log-x fit	log-y fit	log-log fit
Drain-Source Voltage Rating	0.20	0.23	0.21	0.24
Drain Current Rating	0.64	0.74	0.63	0.73
Nominal Threshold Voltage	0.28	0.25	0.28	0.26
$C_{OSS}$ (@1V)	0.32	0.70	0.32	0.69
$C_{ISS}$ (@1V)	0.77	0.83	0.78	0.81
$C_{RSS}$ (@1V)	0.56	0.71	0.56	0.70
Max Power (@25°C)	0.46	0.61	0.47	0.61

Fig. 5. Modulus of Pearson's coefficient of correlation between body diode simplified threshold voltage and MOSFET device parameters.

MOSFET device parameter	linear fit	log-x fit	log-y fit	log-log fit
Drain-Source Voltage Rating	0.68	0.56	0.75	0.7
Drain Current Rating	0.19	0.26	0.36	0.5
Nominal Threshold Voltage	0.32	0.3	0.51	0.51
$C_{OSS}$ (@1V)	0.91	0.77	0.6	0.92
$C_{ISS}$ (@1V)	0.67	0.51	0.74	0.79
$C_{RSS}$ (@1V)	0.73	0.52	0.67	0.75
Max Power (@25°C)	0.44	0.45	0.51	0.79

Fig. 6. Modulus of Pearson's coefficient of correlation between body diode reverse recovery charge and MOSFET device parameters.

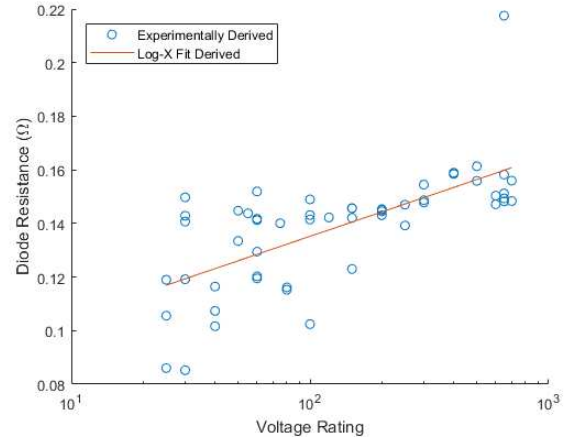


Fig. 7. Body diode forward resistance plotted against and fitted to MOSFET device voltage rating.

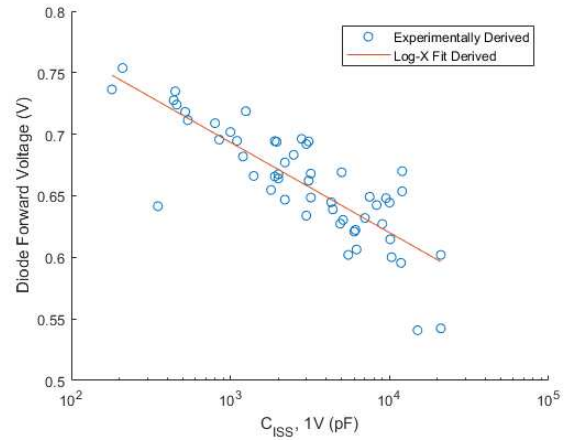


Fig. 8. Body diode simplified threshold voltage plotted against and fitted to MOSFET input capacitance,  $C_{ISS}$ .

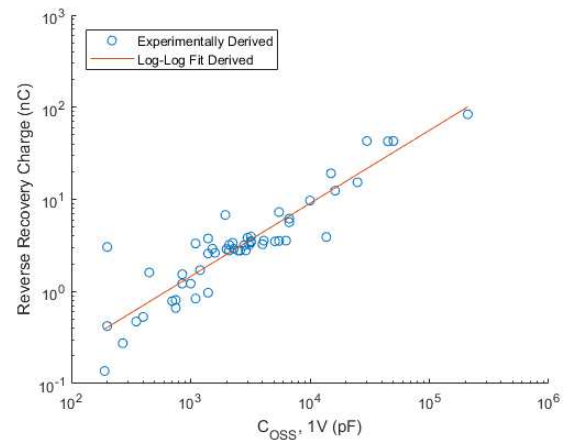


Fig. 9. Body diode reverse recovery charge plotted against and fitted to MOSFET output capacitance,  $C_{OSS}$ .

The expression for the lines of best fit shown in figures 7-9, including numerical coefficients, is shown in figure 10.

$$R_D = 0.0303 \log_{10}(V_{DS,MAX}) + 0.0746$$

$$V_D = -0.0734 \log_{10}(C_{ISS}) + 0.914$$

$$\log_{10}(Q_D) = 0.793 \log_{10}(C_{OSS}) - 11.21$$

Fig. 10. Expressions describing the lines of best fit in figures 7-9.

#### IV. CONCLUSIONS

This research has yielded three key expressions (see figure 10) which permit the estimation of three important performance metrics for MOSFET body diodes in the estimation of power converter loss from readily accessible information. This tool allows for more precise modelling of power converter performance and analysis of large sets of devices with relatively little effort.

Thanks to the testing and analytical methodology any user of these estimations can quote these figures with a defined degree of confidence. This has great utility in the quoting of error bounds for system design.

It also proved interesting to observe which MOSFET device parameters are correlated with certain aspects of body diode performance and which are not. While identifying the causes of these relationships may not be of immediate interest to the authors it could be an interesting area of study nonetheless.

This work could be expanded by similar investigation performed on alternative switching device technologies, such as IGBTs, SiC MOSFETs, GaN HEMTs, etc. This would not only permit similar comparison amongst sets of those devices as this paper has achieved, but also direct comparison in intrinsic body diode performance between different technologies. This would enhance converter design optimisation through device selection further still.

#### REFERENCES

[1] T. Appel and H. G. Eckel, "Bipolar reverse recovery behavior of the body-diode of a SiC JFET," in 2013 15th European Conference on Power Electronics and Applications (EPE), 2013, pp. 1-6.

[2] C. D. Brown and B. Sarlioglu, "Reducing Switching Losses in BLDC Motor Drives by Reducing Body Diode Conduction of MOSFETs," IEEE Transactions on Industry Applications, vol. 51, pp. 1864-1871, 2015.

[3] T. Funaki, "A study on performance degradation of SiC MOSFET for burn-in test of body diode," in 2013 4th IEEE International Symposium on Power Electronics for Distributed Generation Systems (PEDG), 2013, pp. 1-5.

[4] J. Roig, S. Mouhoubi, F. D. Pestel, N. Martens, F. Bauwens, H. Massie, et al., "Body-diode related losses in Shield-Plate FETs for SiP 12V-input DC/DC buck converters operating at high-

frequency (4MHz)," in 2012 24th International Symposium on Power Semiconductor Devices and ICs, 2012, pp. 291-294.

[5] C. Schmidt and M. Roebnitz, "A Performance Comparison of SiC Power Modules with Schottky and Body Diodes," in PCIM Europe 2017; International Exhibition and Conference for Power Electronics, Intelligent Motion, Renewable Energy and Energy Management, 2017, pp. 1-8.

[6] R. Siemieniec, O. Blank, M. Hutzler, L. J. Yip, and J. Sanchez, "Robustness of MOSFET devices under hard commutation of the body diode," in 2013 15th European Conference on Power Electronics and Applications (EPE), 2013, pp. 1-10.

[7] A. Petersen, D. A. Stone, M. P. Foster, and D. T. Gladwin, "Switching Loss Optimisation of Cascaded H-Bridge Converters for Bidirectional Grid-Tie Battery Energy Storage Systems," presented at the IECON 2017, Beijing, 2017.

#### APPENDIX A

List of devices used in testing:

AUIRF1010	IPP200N15	IXFL210N30
AUIRFP4409	IPP320N20	MDP1921
BSC076N06	IPW60R041	MKE38RK600
BSP318S	IRF3315	NVTFS5811
BSZ036NE2	IRF530N	PSMN1R2
BSZ042N04	IRF640	RFD14N05
FCH47N60	IRF740	SI4840
FDBL86210	IRF7493	SPP20N60
FDL100N50	IRF840	SQD50N05
FDMS86255	IRFB4227	SQJA86EP
FDN359AN	IRFML8244	STP16NF06
FDN8601	IRFP064	STP55NF06
FDU3N40	IRFP4229	STY145N65
FQA44N30	IRFP4668	TK40A10
IPA65R280	IRFS7734	TK49N65
IPB034N03	IRFU224	TK72A12
IPB65R045	IRL2703	TPCA8026
IPB65R660	IRL8113	TPCA8048